

Fluorescent Boronic Acid Polymer Grafted on Silica Particles for Affinity Separation of Saccharides

Zhifeng Xu,^{†,‡,§} Khan Mohammad Ahsan Uddin,[†] Tripta Kamra,^{†,#} Joachim Schnadt,[#] and Lei Ye^{*,†}

[†]Division of Pure and Applied Biochemistry, Lund University, Box 124, 221 00 Lund, Sweden

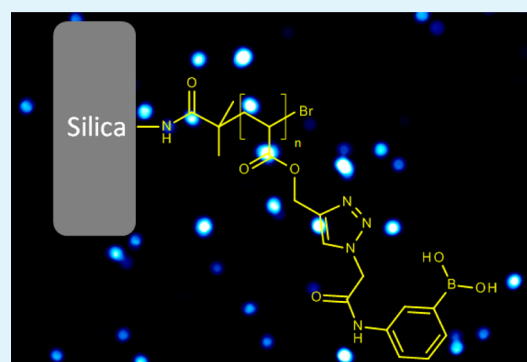
[‡]Department of Chemistry and Material Science, Hengyang Normal University, Hengyang, Hunan 421008, China

[§]Key Laboratory of Functional Organometallic Materials, College of Hunan Province, Hengyang, Hunan 421008, China

[#]Division of Synchrotron Radiation Research, Lund University, Box 118, 221 00 Lund, Sweden

S Supporting Information

ABSTRACT: Boronic acid affinity gels are important for effective separation of biological active cis-diols, and are finding applications both in biotech industry and in biomedical research areas. To increase the efficacy of boronate affinity separation, it is interesting to introduce repeating boronic acid units in flexible polymer chains attached on solid materials. In this work, we synthesize polymer brushes containing boronic acid repeating units on silica gels using surface-initiated atom transfer radical polymerization (ATRP). A fluorescent boronic acid monomer is first prepared from an azide-tagged fluorogenic boronic acid and an alkyne-containing acrylate by Cu(I)-catalyzed 1,3-dipolar cycloaddition reaction (the CuAAC click chemistry). The boronic acid monomer is then grafted to the surface of silica gel modified with an ATRP initiator. The obtained composite material contains boronic acid polymer brushes on surface and shows favorable saccharide binding capability under physiological pH conditions, and displays interesting fluorescence intensity change upon binding fructose and glucose. In addition to saccharide binding, the flexible polymer brushes on silica also enable fast separation of a model glycoprotein based on selective boronate affinity interaction. The synthetic approach and the composite functional material developed in this work should open new opportunities for high efficiency detection, separation, and analysis of not only simple saccharides, but also glycopeptides and large glycoproteins.



KEYWORDS: boronic acid, click chemistry, affinity separation, atom transfer radical polymerization, molecular recognition

1. INTRODUCTION

Carbohydrates exist widely in nature and act as one of the most essential units constituting glycoproteins and nucleic acids. Carbohydrates play important roles in living organisms by acting as structural materials, energy sources, and in controlling cellular communications in different biological processes. For biomedical applications, it is highly desirable that saccharide-sensitive systems can respond selectively under physiological conditions (i.e., in aqueous solution at neutral pH).^{1–6} With their well-known property of forming reversible cyclic ester bond with diols, phenylboronic acids have been utilized to design functional materials for separation and detection of saccharides.^{7–19} The covalent bond formed between phenylboronic acid and the hydroxyl groups of saccharides (1,2- or 1,3-diols) leads to a five- or six-membered ring structure, which is stable under alkaline conditions. Compared to other synthetic receptors that can afford saccharide binding, boronic acid has much higher affinity and provides high flexibility in giving functional materials for separation and sensing of biological cis-diol compounds.

For many practical applications, immobilization on a solid support allows boronic acid to be easily recovered for repeated

use.^{20–22} Boronic acid has also been incorporated into polymers to enable more advanced molecular recognition with functional polymers and supramolecular structures.^{23–28} Also, boron-containing polymers represent an important class of materials that are extensively used, for example, as electrolyte materials, blue emissive polymers, self-healing materials, flame-retardants, and responsive carriers for controlled drug delivery.^{29–34}

Various boronic acid ligands have been developed in the past. The common feature of these ligands is that they contain one boronic acid moiety able to bind *cis*-diols, and one functional group (e.g., amino, thiol, or polymerizable vinyl group) that can be used for immobilization on solid support.^{20,35–38} In a previous work, we developed a clickable boronic acid, 3-(2-azido-acetyl-amino)phenylboronic acid (APBA) by introducing a terminal azide into commercially available 3-aminophenyl boronic acid.²¹ Interestingly, after APBA was conjugated to alkyne-functionalized material via Cu(I)-catalyzed azide–alkyne

Received: June 18, 2013

Accepted: January 20, 2014

Published: January 20, 2014

cycloaddition (CuAAC) click reaction (which changed the terminal azide into a triazole ring),³⁹ the immobilized boronic acid displayed obvious fluorescence response to saccharides.^{21,22} The previous results suggest that the clickable APBA may be conjugated with other vinyl monomers via the same CuAAC click reaction, thereby leading to fluorogenic polymers that can be synthesized by different radical polymerization methods. With boronic acid-based vinyl monomer available, it should be possible to synthesize new functional polymers containing a high density of pendent boronic acid. The presence of multiple boronic acids in a single polymer chain should also be interesting for studying multivalent interactions between saccharides and synthetic polymers.

Because of their mechanical stability, high surface area, and ease of surface functionalization, silica gels have been utilized extensively as solid support for separation purposes, e.g., as stationary phase in liquid chromatography and solid phase extraction. To increase the density of boronic acid ligand on solid support, we are particularly interested in grafting boronic acid-functionalized polymers (polymer brushes) on silica surface. In the literature, grafting of phenylboronic acid polymer has been achieved using free radical polymerization of acrylamidophenylboronic acid in the presence of surface-immobilized chain transfer agent.^{40,41} During the polymerization, the surface-bound transfer agent (mercaptopropyl group) captured some of the growing radicals in solution to give the surface-bound polymer brushes. The disadvantage of this approach is that only a small portion of the monomers can be turned into surface-bound polymer brush. Besides, under traditional radical polymerization condition, it is impossible to control the sequence and molecular weight of the polymer brushes, making it difficult to control the selectivity and the stimuli-response property of the polymer brush. These problems may be addressed by using more sophisticated, surface-initiated, controlled radical polymerization (CRP) techniques, because CRP allows more precise control of polymer structure (in terms of sequence and molecular weight), and surface-initiated CRP only generates polymer brushes on surface with no polymer product in solution. Among the different CRP methods that can be adopted to graft polymer brushes on surface, atom transfer radical polymerization (ATRP) is the most popular, partly because it is straightforward to immobilize ATRP initiator on many different surfaces.^{42–45} Although ATRP can be used to synthesize polymers containing many different functional groups,^{46–48} it remains challenging to achieve direct polymerization of boronic acid-containing monomers by ATRP.²⁹

In this work, we first synthesized a new fluorescent boronic acid monomer (APBA-PA) by conjugating APBA with propargyl acrylate using Cu(I)-catalyzed azide–alkyne cycloaddition (CuAAC) reaction, and grafted a homopolymer of APBA-PA on silica using surface initiated ATRP. The use of CuAAC offered the fluorogenic boronic acid monomer while the surface initiated ATRP made it possible to produce only the surface bound polymer brushes. We characterized the silica–polymer composite using FT-IR, fluorescence microscopy, spectrofluorometry, scanning electron microscopy (SEM), thermogravimetric analysis (TGA), solid-state ¹¹B NMR spectroscopy and X-ray photoelectron spectroscopy (XPS). We also studied the molecular binding characteristics of the composite material and its fluorescence response to fructose and glucose under physiological pH conditions. In addition to binding simple saccharides, we also demonstrate that the

flexible polymer brushes on silica are able to bind large glycoprotein (horseradish peroxidase) through selective boronate affinity interaction.

2. EXPERIMENTAL SECTION

2.1. Materials. Aminopropyl silica gel (particle size 15–35 μm , pore size ~ 9 nm) was purchased from Fluka. Bromoacetyl bromide, 3-aminophenylboronic acid hemisulfate, CuSO_4 , CuBr (98%), sodium ascorbate, sodium azide, tris(2-dimethylaminoethyl)amine (Me_6TREN), Alizarin Red S (ARS), propargyl acrylate, 2-bromoisobutyl bromide, D-fructose, D-glucose, hydrofluoric acid (>40%), methylsulfoxide-*d*₆ (99.9 atom % D), horseradish peroxidase (HRP) (lyophilized powder, ~ 150 U/mg), H_2O_2 solution (30%) and 4-aminoantipyrine were purchased from Sigma-Aldrich. Phenol (99.5%) was obtained from Merck. CuBr was stirred overnight in acetic acid, filtered, washed with acetone and dried in vacuo before use. Tetrahydrofuran (THF), 2-propanol and *N,N*-dimethylformamide (DMF) of analytical grade were purchased from Sigma-Aldrich and used without further purification. Ultrapure water (18.2 M Ω cm) obtained from an ELGA LabWater System (Vivendi Water Systems Ltd.) was used throughout the experiments. APBA was synthesized according to a published procedure.²¹

2.2. Synthesis of Boronic Acid Monomer APBA-PA. APBA (0.219 g, 1.0 mmol) was dissolved in 6 mL of methanol:water (2:1, v/v). To the solution propargyl acrylate (PA, 110 μL , 1.0 mmol), 200 μL of CuSO_4 (100 mM in water) and 3.0 mL of sodium ascorbate (100 mM in water) were added. The solution was purged with a stream of nitrogen gas for 5 min, sealed, and stirred at room temperature for 48 h. After the solvent was removed using a rotary evaporator, the dry product was dissolved in a mixture of ethyl acetate and water (1:1, v/v). The ethyl acetate phase was collected, washed with water, and dried over anhydrous sodium sulfate. After the solvent was removed with a rotary evaporator, the crude product was recrystallized twice from n-hexane: ethyl acetate (1:5, v/v) to give APBA-PA as a pale yellow solid. Yield: 53%. ¹H NMR ($\text{DMSO-}d_6$, 400 MHz): δ 10.41 (broad, 1H, NH), 8.22 (s, 1H, NCH=C), 8.04 (s, 2H, B(OH)₂), 7.29–7.86 (broad, 4H, C₆H₄), 6.36 (d, 1H, COCH=C), 6.22 (broad, 1H, COCH=CH₂), 5.97 (broad, 1H, COCH=CH₂), 5.34 (s, 2H, NHCOCH₂), 5.26 (s, 2H, COOCH₂). ¹³C NMR ($\text{DMSO-}d_6$, 100 MHz): δ 165.7, 164.5, 141.9, 138.0, 132.6, 130.0, 128.5, 128.3, 127.1, 125.7, 121.6, 57.8, 52.6. FT-IR ν (cm^{-1}): 3290, 3144, 1675, 1615, 1548, 1411, 1332, 1175, 1051, 993, 813, 724. Anal. Calcd for C₁₄H₁₅BN₄O₅: C, 50.94; H, 4.58; N, 16.97. Found: C, 51.3; H, 4.80; N, 16.1.

2.3. Immobilization of ATRP Initiator on Silica. Aminopropyl silica (0.5 g) and triethylamine (0.80 mL, 5.8 mmol) were mixed in THF (12 mL) and cooled on an ice–water bath. To the suspension was slowly added 2-bromoisobutyl bromide (1.15 g, 5.0 mmol). The reaction mixture was warmed to room temperature and stirred overnight. The silica particles (Si@initiator) were isolated by centrifugation, washed with water and methanol, and dried in a vacuum chamber.

2.4. Grafting Poly(APBA-PA) on Silica Using Surface-Initiated ATRP. APBA-PA (1.329 g, 4.0 mmol), CuBr (0.0144 g, 0.10 mmol) and 2-propanol (15.0 mL) were added to a 100 mL flask. The mixture was deoxygenated by bubbling with nitrogen gas for 40 min. After addition of Me₆TREN (0.0276 g, 0.12 mmol) through a syringe, the solution was stirred for 20 min to allow formation of the CuBr/Me₆TREN complex. The initiator-immobilized silica gel (0.20 g) was then added to start the polymerization. The reaction mixture was heated at 90 °C and magnetically stirred under nitrogen atmosphere for 48 h. After the reaction, the silica particles modified with poly(APBA-PA) (Si@poly(APBA-PA)) were isolated by centrifugation, and washed thoroughly with water and methanol until no fluorescence emission could be observed from the supernatant.

2.5. Removal of Silica by Hydrofluoric Acid Etching. To remove the silica gel from the composite material, 0.100 g of the poly(APBA-PA) grafted silica particles were transferred into a plastic

tube and stirred in 6.0 mL of hydrofluoric acid: water (1:1) at room temperature for 12 h. After this step, the polymer precipitate was collected by centrifugation, washed with water, methanol, and then dried in a vacuum chamber.

2.6. Measurement of Fluorescence Response to Monosaccharides. To a set of 15 mL calibrated test tubes, 2.0 mg of silica particles, 0.5 mL of 0.20 M phosphate buffer (PBS) (pH 7.4), and a given concentration of saccharide solution were sequentially added. The mixture was then diluted to 2.5 mL with ultrapure water and gently shaken on a rocking table. Fluorescence spectra were collected after 2 h. To maintain a stable particle suspension, the samples were stirred with a built-in magnetic stirrer during the fluorescence measurement.

2.7. Separation of Monosaccharides Using Si@poly(APBA-PA). To a set of 15 mL calibrated test tubes, 3.0 mg of Si@poly(APBA-PA), 0.5 mL of 0.20 M PBS (pH 7.4) and a given concentration of monosaccharide solution were added. The initial concentrations of the monosaccharides were 2.0, 4.0, 6.0, 8.0, and 10.0 mM, respectively. The mixture was then diluted to 3.0 mL with ultrapure water, and gently shaken on a rocking table for 2 h. After the silica particles were removed by centrifugation, the concentration of the monosaccharide in the supernatant was determined using a competition assay as described in our previous publication.²² The amount of fructose bound to the particles was calculated by subtracting the amount of free fructose from the initial amount of fructose added. The results reported were mean values from triplicate independent samples.

2.8. Binding of Glycoprotein with Si@poly(APBA-PA). Horse-radish peroxidase (HRP, 1 mg/mL) was dissolved in 1 mL of buffer containing 3 mg of Si@poly(APBA-PA) particles. The suspension was gently stirred at 20 °C for 1 h and then centrifuged. After removing supernatant, the particles were washed in the same buffer (20 °C, 1 h) two times, and isolated by centrifugation. To test the enzyme activity on the particles, the particles were mixed with 1 mL of freshly prepared substrate solution (obtained by mixing 0.75 mL of 1.7 mM H₂O₂ in 0.1 M PBS buffer at pH 9.0 and 0.7 mL of an aqueous solution of 2.5 mM 4-aminoantipyrine with 0.17 M phenol) and shaken for 2 min. After centrifugation, the particles were removed, and the UV-vis absorption of the supernatant at 510 nm was measured. For comparison, HRP binding to the initiator-modified particles (Si@initiator) was also tested following the same procedure.

2.9. Separation of Glycoprotein Using Si@poly(APBA-PA). Si@poly(APBA-PA) particles (50 mg) were packed into a glass column equipped with a PTFE frit. The particles were conditioned with 0.1 M PBS buffer at pH 9.0 before 2 mL of HRP solution (prepared in the same buffer) was passed through the column at a flow rate of ~1 mL/min. The column was then washed with 2 mL of 0.1 M PBS buffer at pH 9.0 for 2 times. Finally, the bound HRP was eluted with 2 mL of 0.1 M sodium acetate buffer at pH 4.6. The concentration of HRP in the different fractions was calculated from the results of enzyme activity assay as described in the literature.⁴⁹

2.10. Characterization. Attenuated total reflection (ATR) infrared spectra were recorded using a Perkin-Elmer FTIR instrument (Perkin-Elmer Instruments). The fluorescence emission was measured using a QuantaMaster C-60/2000 spectrofluorometer (Photon Technology International, Lawrenceville, NJ, USA). ¹H and ¹³C NMR spectra were recorded on a superconducting magnet NMR spectroscopy 400 MHz (Bruker B-ACS60). Solid-state ¹¹B MAS NMR experiments were performed on a Bruker 500 MHz Avance III instrument in the Chemical Biological Center, Umeå University. X-ray photoelectron spectroscopy (XPS) analysis was carried out using a spectrometer with a Mg K_α (excitation 1253.6 eV) X-ray source. For fluorescence microscopy imaging, samples were deposited on a glass slide and observed under a Nikon Eclipse E400 epifluorescence microscope equipped with a CCD camera. The conditions of measurement were: exposure time: 0.2 s, readout rate: 1 MHz at 16-bit, preamplifier gain: 5×, output amplifier: conventional. Elemental analysis was carried out using a Vario EL CHNS elemental analyzer (Elementar, Germany). The surface morphologies of silica particles were observed with a scanning electron microscope (SEM; JEOLJSM-

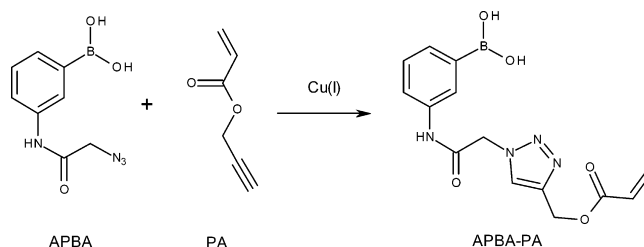
T300). Thermal gravimetric analysis (TGA) was performed in synthetic air using a TGS-2 thermogravimetric analyzer (Perkin-Elmer, USA). The samples were heated from 40 to 700 °C at 10 °C/min and held for 30 min.

3. RESULTS AND DISCUSSION

3.1. Material Synthesis and Characterization. In a previous work, we observed unexpected fluorescence emission of the azide-tagged boronic acid APBA. More importantly, this boronic acid remained the interesting fluorescence property after its azide group was conjugated with an alkyne compound to form a triazole ring.^{21,22} On the basis of these previous results, we considered it possible to use straightforward CuAAC to synthesize APBA-based vinyl monomers by coupling APBA with commercially available alkyne-terminated monomer, e.g., PA. We expected the new monomers and their polymer product to display also favorable fluorescence property and affinity to saccharides similar to APBA.

Synthesis of APBA-PA via CuAAC was straightforward, giving polymerizable boronic acid containing a triazole spacer (Scheme 1). As we expected, APBA-PA displayed fluorescence

Scheme 1. Synthesis of Boronic Acid Monomer APBA-PA



excitation and emission spectra very similar to its precursor APBA. Figure 1 shows that when APBA-PA in methanol was

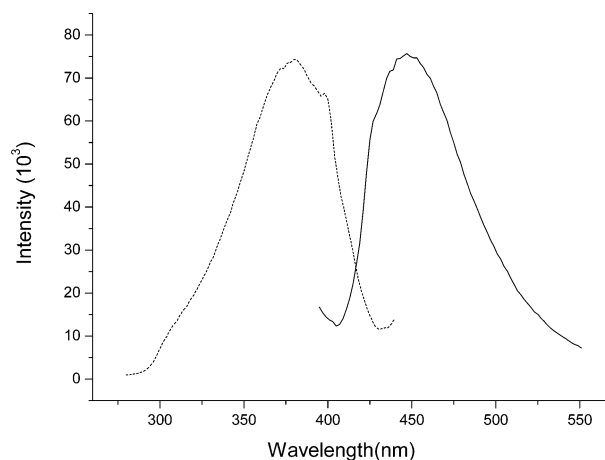
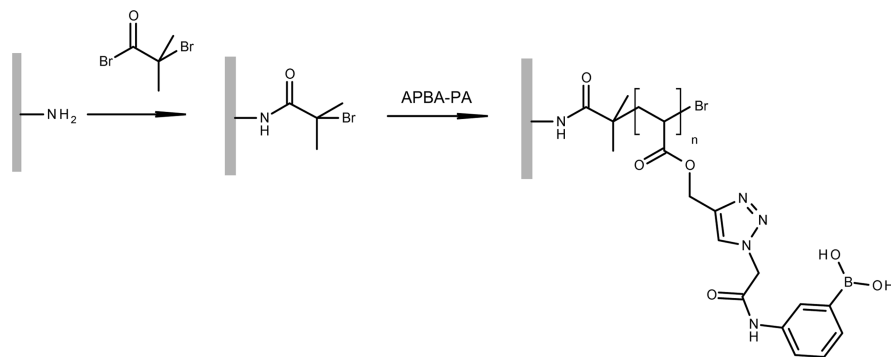


Figure 1. Fluorescence excitation (dotted line) and emission spectra (solid line) of APBA-PA in methanol.

excited at 380 nm, it emitted fluorescence with maximum emission at 447 nm. Using coumarin 343 as a reference,⁵⁰ we estimated the fluorescence quantum yield of APBA-PA in methanol to be 0.08, which is similar to the value of 0.06 for APBA measured in our previous work.²¹

Scheme 2 describes the process of grafting poly(APBA-PA) on silica. First, an ATRP initiator was immobilized by reacting 2-bromoisobutryl bromide with aminopropyl silica. In the

Scheme 2. Synthesis of Poly(APBA-PA) on Silica Using Surface-Initiated ATRP



second step, surface-initiated polymerization of APBA-PA was carried out on the surface of the initiator-modified silica particles.

In Figure 2, FT-IR spectra of the silica particles after different surface modifications are presented. Compared with amino-

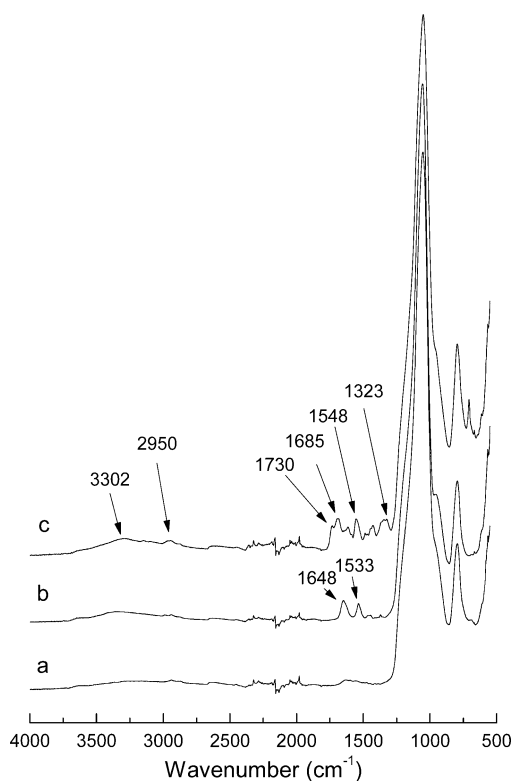


Figure 2. FT-IR spectra of (a) aminopropyl silica, (b) Si@initiator, and (c) Si@poly(APBA-PA).

propyl silica (Figure 2, curve a), the IR spectrum of the initiator-modified silica shows characteristic amide band at 1648 cm^{-1} and amide II band at 1533 cm^{-1} (Figure 2, curve b), confirming that the ATRP initiator has been successfully conjugated to the aminopropyl silica. After the surface-initiated ATRP, the composite silica displayed characteristic IR bands for C–H stretching (2950 cm^{-1}), C=O stretching (1730 cm^{-1} corresponding to ester bonds) and amide (1685 cm^{-1} and 1548 cm^{-1}) (Figure 2, curve c). These new IR bands suggest that new organic polymer has formed on the silica particles.

To provide more unambiguous proof of surface-grafted poly(APBA-PA), we investigated the fluorescence property of

Si@poly(APBA-PA) suspended in methanol. As a control sample, we also measured the fluorescence spectra of the initiator-modified silica particles. As can be seen in Figure 3,

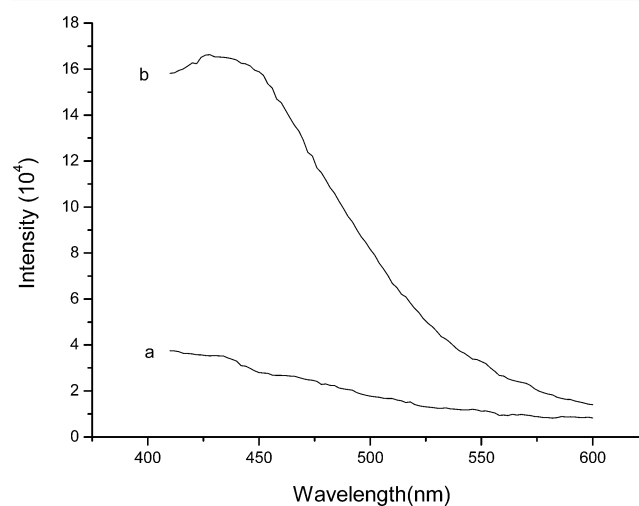


Figure 3. Fluorescence emission spectra of (a) Si@initiator and (b) Si@poly(APBA-PA) in methanol. Particle concentration 1.0 mg/mL , $\lambda_{\text{ex}} = 380\text{ nm}$. To avoid the effect of light scattering caused by the particles, we recorded the emission spectra in the range of 400–600 nm.

Si@poly(APBA-PA) emitted strong fluorescence at 433 nm when it was excited at 380 nm. Compared to the monomer APBA-PA, the maximum fluorescence emission of the surface-grafted poly(APBA-PA) upshifted by 14 nm. The shorter emission wavelength of the polymer may be explained as the following: when APBA-PA was incorporated into the polymer brushes, the fluorophore was moved into a less polar environment because of the presence of the polymer backbone, thereby leading to an upshifted emission. In contrast to Si@poly(APBA-PA), the initiator-modified silica displayed almost no fluorescence emission. On the basis of the strong fluorescence emission, we can conclude that poly(APBA-PA) has been successfully grafted on silica through the surface-initiated ATRP. Si@poly(APBA-PA) particles were also imaged with a fluorescent microscope and compared with the initiator-modified silica. From Figure 4, it is clear that the polymer-modified silica particles are fluorescent because of the boronic acid polymer grafted on the surface.

The SEM image in Figure 5a reveals that the surface grafted poly(APBA-PA) formed aggregates on silica under desolvated condition. The surface morphology of the composite Si@

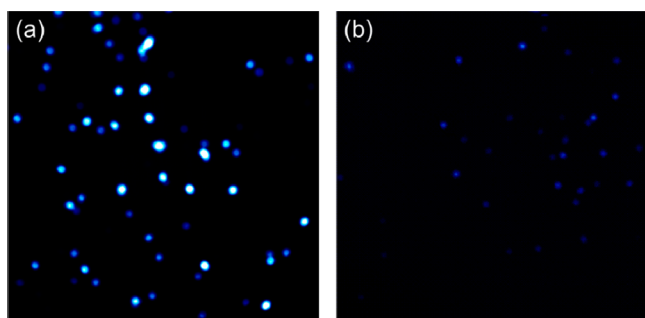


Figure 4. Fluorescence microscope images of (a) Si@poly(APBA-PA) and (b) Si@initiator. The maximum fluorescence intensity was (a) 6.5×10^5 and (b) 6.7×10^4 .

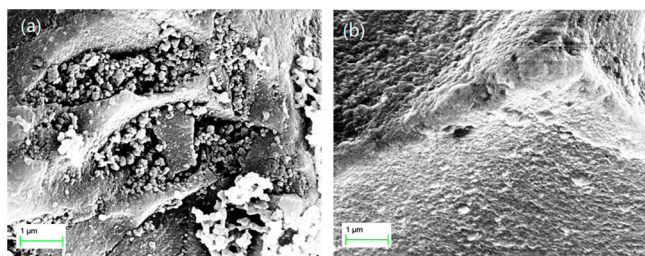


Figure 5. SEM images of (a) Si@poly(APBA-PA) and (b) Si@initiator.

poly(APBA-PA) particles is very different from the initiator-modified silica (that has a much smoother surface, Figure 5b). The significant change of the surface morphology after the ATRP suggests that poly(APBA-PA) has been grafted on silica. The aggregates observed in Figure 5a can be explained as collapsed polymer chains under the desolvated condition.

To further prove the proposed boronic acid structure in Si@poly(APBA-PA) particles, we analyzed the composite material using solid state ^{11}B MAS NMR. As shown in Figure S1 in the Supporting Information, the ^{11}B spectrum has one broad signal at around 18 ppm and one signal close to 0 ppm, which can be assigned to the three- and four-coordinated boron atoms in the polymer brush, respectively. The pattern of this ^{11}B spectrum is in agreement with that of poly(4-vinylbenzylboronic acid) reported in the literature.⁵¹ From the XPS results shown in Figure S2 in the Supporting Information, it is clear that after poly(APBA-PA) was grafted, the N 1s signal from the particles increased significantly. In Figure 6a, the O 1s signal from Si@poly(APBA-PA) is contributed by two types of O atoms in the

ester (532 eV) and in the boronic acid structure (534 eV).^{52,53} The C 1s signal from the composite particles can be fitted with five peaks with binding energies at 284, 285, 286.2, 287.5, and 289 eV, corresponding to aromatic C, aliphatic C, O=C–N in amide, O=C–O in ester, and C–O, respectively (Figure 6b).^{52,54} Although the XPS signals from B 1s and Br 3p overlap in the range of 180–195 eV, making it impossible to distinguish these two elements, the collective results from the solid-state ^{11}B NMR and XPS analyses indicate clearly that poly(APBA-PA) has been successfully grafted on the silica particles.

In a previous work, we showed that a boronic acid-functionalized ATRP initiator failed to produce boronic acid-terminated polyNIPAm.²² Compared to the previous work, the successful synthesis of poly(APBA-PA) using surface-initiated ATRP suggests that the structure of the initiator plays an important role. The major difference between these two systems is that the previous ATRP initiator was linked to a phenylboronic acid through a flexible spacer. Considering possible intramolecular hydrogen bond, it may be that the boronic acid moiety in the previous system could be located very close to the terminal bromide, which generated significant steric hindrance for initiating the ATRP.

To determine the content of the organic polymer in Si@poly(APBA-PA), we used hydrofluoric acid to etch the silica gel from 100 mg of the composite material. This treatment left 29.4 mg of polymer, implying that the polymer content in Si@poly(APBA-PA) was $\sim 29.4\%$.

The results of elemental analysis for the different materials are listed in Table 1. On the basis of the nitrogen content in the

Table 1. Elemental Analysis Results

	C (%)	H (%)	N (%)
aminopropyl silica	5.27	1.19	1.22
Si@initiator	7.72	1.37	1.11
Si@poly(APBA-PA)	16.07	1.94	4.31

aminopropyl silica, we estimated the density of aminopropyl group on the aminopropyl silica to be ~ 0.871 mmol/g. Table 1 shows that immobilization of the ATRP initiator resulted in an obviously increased content of C and H, whereas the content of N slightly decreased. This result can be explained by that the ATRP initiator has a high C and H content, but has no N in its structure. The content of C, H, and N further increased after APBA-PA was graft-polymerized on the silica surface. The obviously higher N content in Si@poly(APBA-PA) than in the other two types of silica particles can be easily explained: the

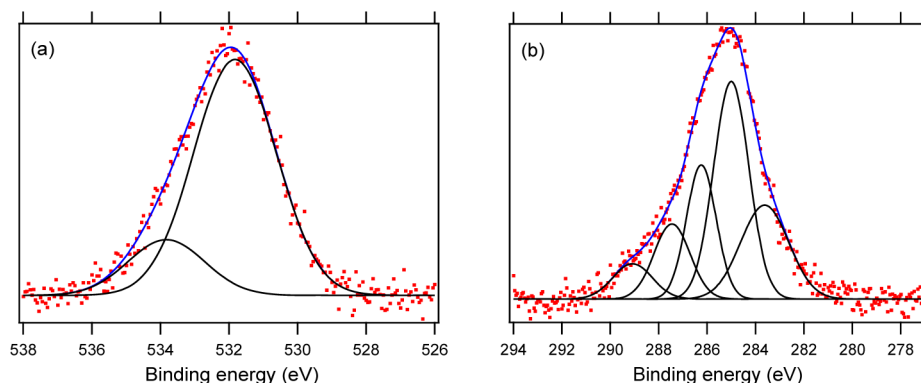


Figure 6. Characterization of Si@poly(APBA-PA) by XPS analysis. Photoelectron spectrum of (a) O 1s and (b) C 1s.

boronic acid monomer has three N atoms in the triazole spacer and one N atom in the amide group, which after polymerization caused the higher N content in the composite material.

The content of organic materials in the three different silica particles was further investigated by TGA analysis. In Figure 7,

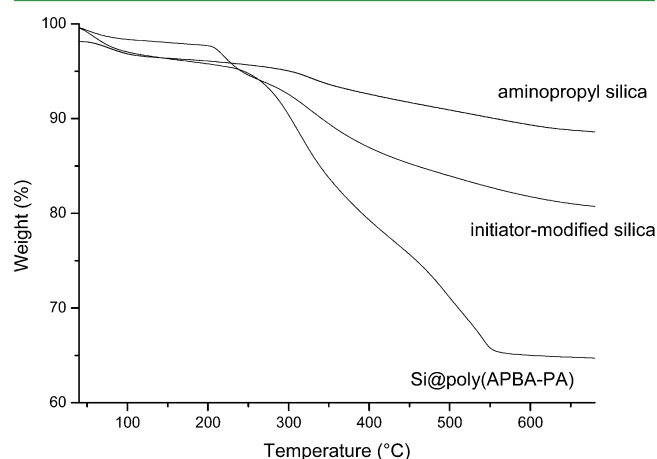


Figure 7. TGA analysis of the different silica particles.

the weight loss (approximately 4%) below 250 °C can be attributed to the evaporation of residual organic solvent and water. The weight loss in the temperature range of 250–550 °C can be attributed to the thermal degradation of the organic materials. Because the weight loss of the aminopropyl silica and the initiator-modified silica in this temperature range were 11.7 and 19.7%, respectively, the density of the initiator immobilized on the silica particles was calculated to be 0.637 mmol/g. Considering the abundance of aminopropyl group on the silica support was ~ 0.871 mmol/g, we found that $\sim 73.1\%$ of the amino groups on the silica support could be converted into surface-bound ATRP initiators.

The TGA curve for Si@poly(APBA-PA) in Figure 7 shows a major decomposition in the temperature range of 250–550 °C, which can be attributed to the thermal degradation of the boronic acid polymer grafted on the silica. When the temperature reached 700 °C, the residual weight was 64.7%. Thus, the polymer content in Si@poly(APBA-PA) can be calculated to be 31.2%. This value is close to that obtained by etching the composite material with hydrofluoric acid (29.4%). Based on these TGA results, the content of the boronic acid monomer (APBA-PA) in the composite Si@poly(APBA-PA) particles can be estimated to be ~ 0.781 mmol/g. Considering that the density of the immobilized ATRP initiator on the silica was 0.637 mmol/g, we can conclude that the ATRP took place only from a small fraction of the surface-immobilized initiator sites. This result is in agreement with the nonuniform polymer grafting on silica observed in the SEM image of Si@poly(APBA-PA) (Figure 5a).

3.2. Effect of pH on *cis*-Diol Binding. Previously, we proposed that the triazole ring connecting the fluorogenic APBA with an alkyne compound can maintain a dative N–B bond, making the conjugated product able to bind saccharides under neutral pH condition.^{21,22} To study the impact of pH on saccharide binding, we took the advantage of the immobilized polymer brush (allowing easy separation), and the fact that ARS can form covalent bond with phenylboronic acid within a relatively broad pH range.⁵⁵ To confirm that ARS binding to APBA-PA is insensitive to pH variation, we first incubated Si@

poly(APBA-PA) with ARS in different buffers. After separating the particles by centrifugation, the supernatant was diluted with 0.1 M PBS (pH 7.4) before its UV–vis absorption was measured. As shown in Figure S3 in the Supporting Information, the uptake of ARS ($\sim 90\%$) by Si@poly(APBA-PA) is almost constant within the range of pH 4.6–9.0. Following this verification, we designed a simple displacement experiment in which we tested if high concentration of fructose can disrupt the binding between ARS and the APBA-PA units. In these experiments, we utilized the fact that binding of ARS to phenylboronic acid is accompanied by a strong fluorescence emission. If fructose can disrupt the covalent bond, it will cause the fluorescence intensity to decrease. Thus the reduction of fluorescence intensity can be used to estimate the potency of fructose to displace ARS from APBA-PA in solution. Figure 8a–c show the effect of adding fructose into a solution of ARS and APBA-PA at different pH values. At pH 4.6, fructose only caused a small reduction of the fluorescence intensity (Figure 8a). At pH 7.4 and 9.0, addition of the same amount of fructose almost completely diminished the fluorescence (Figure 8b, c), indicating nearly quantitative disruption of the ARS: APBA-PA complex. On the basis of these results, we can conclude that saccharide binding with APBA-PA (and the corresponding polymer brush) is favored under neutral and basic conditions, but not under acidic condition.

3.3. Fluorescence Responses of Si@poly(APBA-PA). In previous studies, we have shown that the fluorescence intensity of APBA increases after it binds *cis*-diol compounds.²¹ To investigate if this kind of fluorescence response to *cis*-diol compounds remains after APBA is linked to PA, we measured the fluorescence spectra of Si@poly(APBA-PA) in PBS buffer (pH 7.4) in the presence of different amount of fructose and glucose. Figure 9 shows the change of fluorescence emission of Si@poly(APBA-PA) when increasing amount of fructose and glucose was added into a suspension of Si@poly(APBA-PA) in PBS buffer. Clearly, the intensity of fluorescence emission of the particles increased with the increasing of fructose and glucose concentration. This result confirms that the fluorescence response remains after the terminal azide of APBA was changed into the triazole structure of APBA-PA, which is in agreement with our previous results.^{21,22} The increased fluorescence caused by saccharide can be explained as a result of the dative B–N bond^{56,57} that is stabilized by *cis*-diol binding. From Figure 9, we can see that the degree of fluorescence enhancement caused by fructose is higher than glucose. This phenomenon can be explained by the fact that fructose binds to phenylboronic acid with an affinity higher than glucose.¹¹ It is worth to note that in this work, the corresponding fluorescence response was observed under physiological pH conditions, which makes the fluorescence-responsive materials more suitable for direct analysis of biological samples.

3.4. Separation of Monosaccharides Using Si@poly(APBA-PA). By immobilizing poly(APBA-PA) on silica particles, it becomes straightforward to separate saccharides using simple filtration or centrifugation. The capability of using Si@poly(APBA-PA) to separate monosaccharide was investigated using fructose as a model through equilibrium binding experiments. The binding isotherm of fructose to Si@poly(APBA-PA) was examined using different fructose concentrations in the range of 0–10.0 mM. After equilibrium binding, the silica particles were settled by centrifugation. The concentration of fructose in the supernatant was then

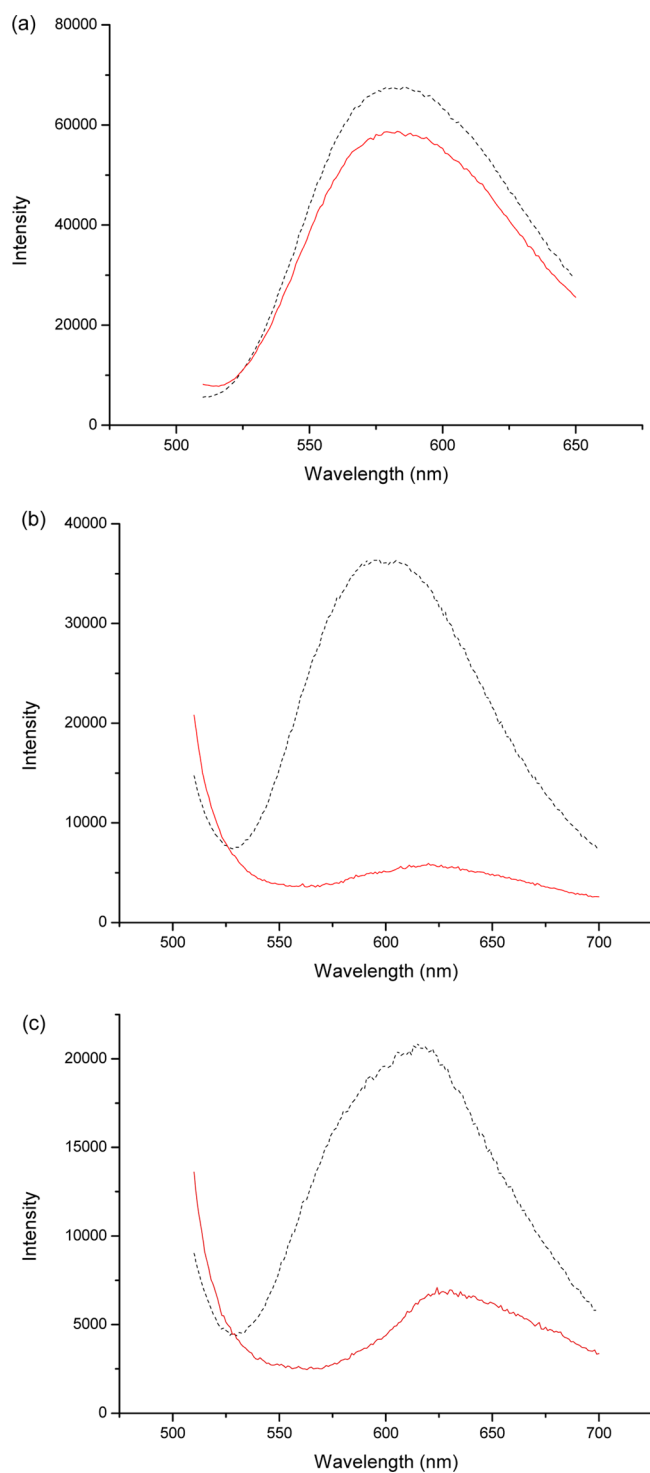


Figure 8. Displacement of ARS from APBA-PA by fructose in (a) 0.1 M acetate buffer, pH 4.6; (b) 0.1 M PBS, pH 7.4; (c) and 0.1 M PBS, pH 9.0. The dotted line represents the fluorescence of a solution containing 0.1 mM ARS and 0.1 mM APBA-PA at the given pH. The solid line represents the fluorescence of the same solution after addition of fructose powder (final concentration 100 mM).

determined through a three-component competitive assay, where the fructose caused a dose-dependent reduction of fluorescence intensity of a mixture of ARS and 3-aminophenylboronic acid).²² The amount of fructose bound to Si@poly(APBA-PA) was then calculated by subtracting the concentration of free fructose from the initial fructose

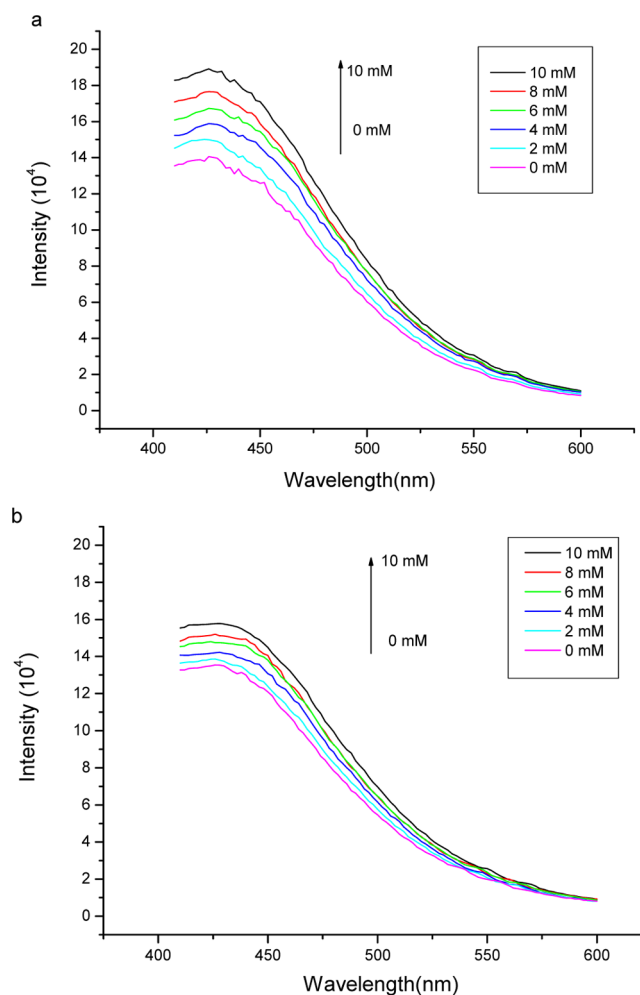


Figure 9. Fluorescence spectra of Si@poly(APBA-PA) (0.80 mg/mL) in 50 mM PBS buffer, pH 7.4, measured in the presence of different amounts of (a) fructose and (b) glucose. $\lambda_{\text{ex}} = 374$ nm.

concentration. For comparison, the initiator-modified silica was used as a control to evaluate the nonspecific binding caused by the silica matrix. As shown in Figure 10, the amount of fructose bound to Si@poly(APBA-PA) increased with the increasing concentration of fructose. The binding reached saturation when the initial concentration of fructose was 6.0 mM, which corresponds to a maximum binding capacity of 0.49

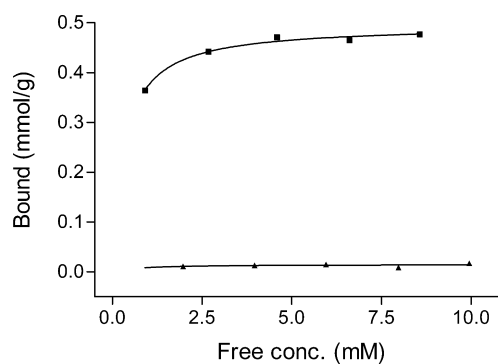


Figure 10. Affinity binding of fructose by poly(APBA-PA) grafted silica (■) and initiator-immobilized silica (▲). Standard deviation of saccharide binding ≤ 0.015 mmol/g ($n = 3$).

mmol/g of Si@poly(APBA-PA). In contrast, the initiator-modified silica particles did not show obvious fructose binding. Therefore, it is clear that the saccharide binding to composite Si@poly(APBA-PA) particles is contributed by the specific interaction between the saccharide and the surface-grafted boronic acid polymer. Although the reported value of saccharide binding is moderate, it should be possible to use ATRP to produce longer polymer brushes so that the binding capacity can be further increased. In addition, surface-initiated ATRP may also be used to prepare copolymer brushes containing an optimal boronic acid sequence and density, which are important for achieving multidentate binding to oligosaccharides and glycoproteins.

3.5. Glycoprotein Separation. Besides binding simple monosaccharides, we also expected the boronic acid polymer brush immobilized on silica to offer a convenient tool for separation of large biomolecules containing *cis*-diols, e.g., glycoproteins. To test this possibility, we selected horseradish peroxidase (HRP) as a model to find out if Si@poly(APBA-PA) can separate this glycoprotein from solution. Using HRP as a model also allows us to investigate if the enzyme remains catalytically active after binding to the polymer brush. In the first experiment, Si@poly(APBA-PA) and Si@initiator were incubated with HRP in two different buffers at pH 4.6 and 9.0. After washing with the same incubation buffer, the particles were separated and mixed with a solution of HRP substrate for 2 min. The absorption at 510 nm in the supernatant was immediately measured after removing the solid particles. Figure 11 shows the results of the colorimetric assay obtained from the two types of particles. Clearly, the highest enzyme activity was observed from Si@poly(APBA-PA) that has been loaded with HRP at pH 9.0. When the incubation was carried out under acidic condition (pH 4.6), the enzyme activity observed from Si@poly(APBA-PA) was very low, suggesting that HRP binding under this condition is negligible. It should be noted that when

the same supernatant was measured for several times, its absorption did not change, indicating that no enzyme detached from the particles during the 2 min reaction time. In comparison with Si@poly(APBA-PA), the more hydrophobic Si@initiator particles displayed high nonspecific binding that was hardly affected by pH variation (Figure 11). As HRP binding with Si@poly(APBA-PA) in the acidic buffer (0.1 M acetate, pH 4.6) is very low, it is possible to use this buffer to recover the bound glycoprotein from the immobilized polymer brushes.

Selective glycoprotein separation was then demonstrated in a column mode. Si@poly(APBA-BA) particles (50 mg) were packed in a solid phase extraction (SPE) column and conditioned with 0.1 M PBS buffer at pH 9.0. After passing through 2 mL of HRP in the basic buffer (1 mg/mL), the column was washed with 2 volumes of the same buffer. The bound HRP was finally eluted in 2 mL of 0.1 M acetate buffer at pH 4.6. All the liquid fractions collected were subjected to enzyme assay to determine the protein concentration. Under the SPE conditions used, we found that ~60% of the initially loaded HRP could be recovered in the elution step, corresponding to a capacity of ~24 mg HRP/g particles. Apparently, the immobilized boronic acid polymer brush has played the important role of capturing the glycoprotein from solution.

4. CONCLUSIONS

In this work, we have grafted fluorogenic boronic acid polymer on silica using surface initiated ATRP. A fluorogenic boronic acid monomer was first synthesized by conjugation of azide-terminated phenylboronic acid with propargyl acrylate through CuAAC. Amino-functionalized silica particles were used to anchor ATRP initiator, which were used directly to graft the fluorogenic boronic acid polymer. While the use of CuAAC offered the fluorogenic boronic acid monomer, the surface-initiated ATRP made it possible to produce only the surface bound polymer brushes. The composite material obtained maintained the fluorogenic property of the monomer, and allowed monosaccharides to be easily separated from solution under physiological pH condition. Because the composite particles have a high density of boronic acids appended on flexible polymer chains, the affinity material could also be used to achieve fast separation of glycoprotein. On the basis of the results obtained in this work, we believe it possible to employ ATRP to further control the architecture and sequence of boronic acid polymer on surface, which should lead to improved molecular selectivity of boronic acid-based affinity materials. The synthetic approach and the composite functional material developed in this work should open new opportunities for high efficiency detection, separation, and analysis of not only simple saccharides but also glycopeptides and large glycoproteins.

■ ASSOCIATED CONTENT

Supporting Information

Solid-state ^{11}B MAS NMR, XPS spectra of N 1s of the different materials, and UV-vis spectra of ARS solutions before and after treatment with Si@poly(APBA-PA). This material is available free of charge via the Internet at <http://pubs.acs.org>.

■ AUTHOR INFORMATION

Corresponding Author

*E-mail: Lei.Ye@tbiokem.lth.se. Tel.: 00 46 46 2229560.

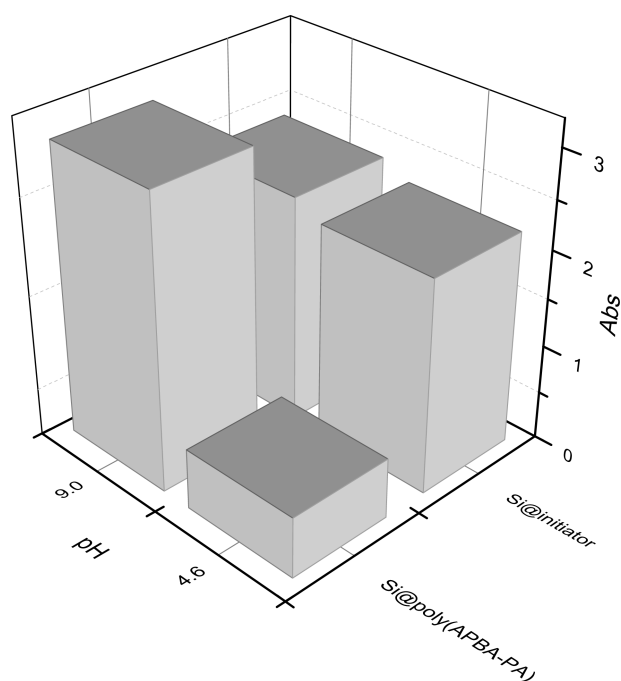


Figure 11. Activity of HRP on particles as estimated from UV-vis absorption of the liquid phase. Standard deviation of Abs ≤ 0.024 ($n = 3$).

Notes

The authors declare no competing financial interest.

ACKNOWLEDGMENTS

This work was supported by the Swedish Research Council FORMAS and the Danish Council for Strategic Research (project FENAMI, DSF-10-93456). Z.X. acknowledges the Open Fund for Key Laboratory of Functional Organometallic Materials for universities in Hunan (No. 12K125), China. We thank Prof. Oliver Brüggemann, Johannes Kepler University Linz, Austria for the TGA analysis, and Dr. Tobias Sparrman, Chemical Biological Center, Umeå University for the solid state ^{11}B NMR analysis through the “NMR for Life” service.

REFERENCES

- (1) Bull, S. D.; Davidson, M. G.; van den Elsen, J. M. H.; Fossey, J. S.; Jenkins, A. T. A.; Jiang, Y.-B.; Kubo, Y.; Marken, F.; Sakurai, K.; Zhao, J.; James, T. D. *Acc. Chem. Res.* **2013**, *46*, 312–326.
- (2) Kim, K. T.; Cornelissen, J. J. L. M.; Nolte, R. J. M.; van Hest, J. C. M. *J. Am. Chem. Soc.* **2009**, *131*, 13908–13909.
- (3) Tuma, P.; Malkova, K.; Samcova, E.; Stulik, K. *Anal. Chim. Acta* **2011**, *698*, 1–5.
- (4) Okutucu, B.; Önal, S.; Telefoncu, A. *Talanta* **2009**, *78*, 1190–1193.
- (5) Lee, J.-D.; Greene, N. T.; Rushton, G. T.; Shimizu, K. D.; Hong, J.-I. *Org. Lett.* **2005**, *7*, 963–966.
- (6) Yang, Y.; Yi, C.; Luo, J.; Liu, R.; Liu, J.; Jiang, J.; Liu, X. *Biosens. Bioelectron.* **2011**, *26*, 2607–2612.
- (7) Shoji, E.; Freund, M. S. *J. Am. Chem. Soc.* **2002**, *124*, 12486–12493.
- (8) Gao, S.; Wang, W.; Wang, B. *Bioorg. Chem.* **2001**, *29*, 308–320.
- (9) Nishiyabu, R.; Kubo, Y.; James, T. D.; Fossey, J. S. *Chem. Commun.* **2012**, *47*, 1106–1123.
- (10) Schumacher, S.; Grüneberger, F.; Katterle, M.; Hettrich, C.; Hall, D. G.; Scheller, F. W.; Gajovic-Eichelmann, N. *Polymer* **2011**, *52*, 2485–2491.
- (11) Tan, J.; Wang, H.-F.; Yan, X.-P. *Anal. Chem.* **2009**, *81*, 5273–5280.
- (12) Manju, S.; Hari, P. R.; Sreenivasan, K. *Biosens. Bioelectron.* **2010**, *26*, 894–897.
- (13) Cao, H.; McGill, T.; Heagy, M. D. *J. Org. Chem.* **2004**, *69*, 2959–2966.
- (14) Edwards, N. Y.; Sager, T. W.; McDevitt, J. T.; Anslyn, E. V. *J. Am. Chem. Soc.* **2007**, *129*, 13575–13583.
- (15) Deng, G.; James, T. D.; Shinkai, S. *J. Am. Chem. Soc.* **1994**, *116*, 4567–4512.
- (16) Zhu, W.; Wu, F. *Prog. Chem.* **2009**, *21*, 1241–1253.
- (17) Ishi-i, T.; Iguchi, R.; Shinkai, S. *Tetrahedron* **1999**, *55*, 3883–3892.
- (18) Inoue, K.; Ono, Y.; Kanekiyo, Y.; Ishi-i, T.; Yoshihara, K.; Shinkai, S. *Tetrahedron Lett.* **1998**, *39*, 2981–2984.
- (19) Roy, D.; Sumerlin, B. S. *ACS Macro Lett.* **2012**, *1*, 529–532.
- (20) Suksrichavalit, T.; Yoshimatsu, K.; Prachayasittikul, V.; Bülow, L.; Ye, L. *J. Chromatogr., A* **2010**, *1217*, 3635–3641.
- (21) Uddin, K. M. A.; Ye, L. *J. Appl. Polym. Sci.* **2013**, *128*, 1527–1533.
- (22) Xu, Z.; Uddin, K. M. A.; Ye, L. *Macromolecules* **2012**, *45*, 6464–6470.
- (23) De, P.; Gondi, S. R.; Roy, D.; Sumerlin, B. S. *Macromolecules* **2009**, *42*, 5614–5621.
- (24) Bench, B. J.; Johnson, R.; Hamilton, C.; Gooch, J.; Wright, J. R. *J. Colloid Interface Sci.* **2004**, *270*, 315–320.
- (25) Roy, D.; Cambre, J. N.; Sumerlin, B. S. *Chem. Commun.* **2008**, 2477–2479.
- (26) Cambre, J. N.; Sumerlin, B. S. *Polymer* **2011**, *52*, 4631–4643.
- (27) Cambre, J. N.; Roy, D.; Gondi, S. R.; Sumerlin, B. S. *J. Am. Chem. Soc.* **2007**, *129*, 10348–10349.
- (28) Wang, B.; Ma, R.; Liu, G.; Li, Y.; Liu, X.; An, Y.; Shi, L. *Langmuir* **2009**, *25*, 12522–12528.
- (29) Qin, Y.; Sukul, V.; Pagakos, D.; Cui, C.; Jäkle, F. *Macromolecules* **2005**, *38*, 8987–8990.
- (30) Niu, W.; O’Sullivan, C.; Rambo, B. M.; Smith, M. D.; Lavigne, J. *J. Chem. Commun.* **2005**, 4342–4344.
- (31) Niu, W.; Smith, M. D.; Lavigne, J. J. *J. Am. Chem. Soc.* **2006**, *128*, 16466–16467.
- (32) Tilford, R. W.; Gemmill, W. R.; Loye, H.-C. Z.; Lavigne, J. J. *Chem. Mater.* **2006**, *18*, 5296–5301.
- (33) Jäkle, F. *Chem. Rev.* **2010**, *110*, 3985–4022.
- (34) Jay, J. I.; Shukair, S.; Langheinrich, K.; Hanson, M. C.; Cianci, G. C.; Johnson, T. J.; Clark, M. R.; Hope, T. J.; Kiser, P. F. *Adv. Funct. Mater.* **2009**, *19*, 2969–2977.
- (35) Preinerstorfer, B.; Lämmerhofer, M.; Linder, W. *J. Sep. Sci.* **2009**, *32*, 1673–1685.
- (36) Foettinger, A.; Leitner, A.; Linder, W. *J. Chromatogr. A* **2005**, *1079*, 187–196.
- (37) Pereira Morais, M. P.; Mackay, J. D.; Bhamra, S. K.; Buchanan, J. G.; James, T. D.; Fossey, J. S.; van den Elsen, J. M. H. *Proteomics* **2010**, *10*, 48–58.
- (38) Jackson, T. R.; Springall, J. S.; Rogalle, D.; Masumoto, N.; Ching Li, H.; D’Hooge, F.; Perera, S. P.; Jenkins, T. A.; James, T. D.; Fossey, J. S.; van den Elsen, J. M. H. *Electrophoresis* **2008**, *29*, 4185–4191.
- (39) Kolb, H. C.; Finn, M. G.; Sharpless, K. B. *Angew. Chem., Int. Ed.* **2001**, *40*, 2004–2021.
- (40) Ivanov, A. E.; Eccles, J.; Panahi, H. A.; Kumar, A.; Kuzimenkova, M. V.; Nilsson, L.; Bergenstahl, B.; Long, N.; Philips, G. J.; Mikhailovsky, S. V.; Galaev, I.; Mattiasson, B. *J. Biomed. Mater. Res.* **2009**, *88A*, 213–225.
- (41) Liu, H.; Li, Y.; Sun, K.; Fan, J.; Zhang, P.; Meng, J.; Wang, S.; Jiang, L. *J. Am. Chem. Soc.* **2013**, *135*, 7603–7609.
- (42) Coessens, V.; Pintauer, T.; Matyjaszewski, K. *Prog. Polym. Sci.* **2001**, *26*, 337–77.
- (43) Pyun, J.; Matyjaszewski, K. *Chem. Mater.* **2001**, *13*, 3436–48.
- (44) Siegwart, D. J.; Oh, J. K.; Matyjaszewski, K. *Prog. Polym. Sci.* **2012**, *37*, 18–37.
- (45) Couet, J.; Biesalski, M. *Macromolecules* **2006**, *39*, 7258–7268.
- (46) Matyjaszewski, K.; Xia, J. *Chem. Rev.* **2001**, *101*, 2921–2990.
- (47) Kamigaito, M.; Ando, T.; Sawamoto, M. *Chem. Rev.* **2001**, *101*, 3689–3745.
- (48) Jiang, J.; Zhang, Y.; Guo, X.; Zhang, H. *Macromolecules* **2011**, *44*, 5893–5904.
- (49) Hajizadeh, S.; Kirsebom, H.; Leistner, A.; Mattiasson, B. *J. Sep. Sci.* **2012**, *35*, 2978–2985.
- (50) Reynolds, G. A.; Drexhage, K. H. *Opt. Commun.* **1975**, *13*, 222–225.
- (51) Sezgin, A.; Akbey, Ü.; Hansen, M. R.; Graf, R.; Bozkurt, A.; Baykal, A. *Polymer* **2008**, *49*, 3859–3864.
- (52) De’Nève, B.; Delamar, M.; Nguyen, T. T.; Shanahan, M. E. R. *Appl. Surf. Sci.* **1998**, *134*, 202–212.
- (53) Joyner, D. J.; Hercules, D. M. *J. Chem. Phys.* **1980**, *72*, 1095–1108.
- (54) Vandencastele, N.; Reniers, F. J. *Electron Spectrosc. Relat. Phenom.* **2010**, *178–179*, 394–408.
- (55) Springsteen, G.; Wang, B. *Chem. Commun.* **2001**, 1608–1609.
- (56) Larkin, J. D.; Fossey, J. S.; James, T. D.; Brooks, B. R.; Bock, C. W. *J. Phys. Chem.* **2010**, *114*, 12531–12539.
- (57) Collins, B. E.; Sorey, S.; Hargrove, A. E.; Shabbir, S. H.; Lynch, V. M.; Anslyn, E. V. *J. Org. Chem.* **2009**, *74*, 4055–4060.